Research Article

Inhalation of panaxadiol alleviates lung inflammation *via* inhibiting TNFA/TNFAR and IL7/IL7R signaling between macrophages and epithelial cells

Yifan Wang [a,#], Hao Wei [a,b,#], Zhen Song [c,#], Liqun Jiang [b], Mi Zhang [b], Xiao Lu [d], Wei Li [d], Yuqing Zhao [d], Lei Wu [a], Shuxian Li [a], Huijuan Shen [e], Qiang Shu [a,*], Yicheng Xie [a,*]

[a] *Department of Pulmonology, Children's Hospital, Zhejiang University School of Medicine, National Clinical Research Center for Child Health, Hangzhou, China*
[b] *Department of Pharmacy, Xuzhou Medical University, Xuzhou, China*
[c] *Department of Molecular Bioinformatics, Institute of Computer Science, Goethe University Frankfurt, Frankfurt am Main, Germany*
[d] *Shenyang Pharmaceutical University, Shenyang, China*
[e] *The Second Affiliated Hospital, Zhejiang University School of Medicine, Hangzhou, China*

ARTICLE INFO

ABSTRACT

Background: Lung inflammation occurs in many lung diseases, but has limited effective therapeutics. Ginseng and its derivatives have anti-inflammatory effects, but their unstable physicochemical and metabolic properties hinder their application in the treatment. Panaxadiol (PD) is a stable saponin among ginsenosides. Inhalation administration may solve these issues, and the specific mechanism of action needs to be studied.
Methods: A mouse model of lung inflammation induced by lipopolysaccharide (LPS), an in vitro macrophage inflammation model, and a coculture model of epithelial cells and macrophages were used to study the effects and mechanisms of inhalation delivery of PD. Pathology and molecular assessments were used to evaluate efficacy. Transcriptome sequencing was used to screen the mechanism and target. Finally, the efficacy and mechanism were verified in a human BALF cell model.
Results: Inhaled PD reduced LPS-induced lung inflammation in mice in a dose-dependent manner, including inflammatory cell infiltration, lung tissue pathology, and inflammatory factor expression. Meanwhile, the dose of inhalation was much lower than that of intragastric administration under the same therapeutic effect, which may be related to its higher bioavailability and superior pharmacokinetic parameters. Using transcriptome analysis and verification by a coculture model of macrophage and epithelial cells, we found that PD may act by inhibiting TNFA/TNFAR and IL7/IL7R signaling to reduce macrophage inflammatory factor-induced epithelial apoptosis and promote proliferation.
Conclusion: PD inhalation alleviates lung inflammation and pathology by inhibiting TNFA/TNFAR and IL7/IL7R signaling between macrophages and epithelial cells. PD may be a novel drug for the clinical treatment of lung inflammation.

1. Introduction

Ginseng is considered one of the most widely consumed herbal products worldwide and plays an important role in maintaining homeostasis, combating fatigue, relieving stress, reducing stress, etc. [1,2]. Triterpene glycosides, also known as ginsenosides, are the primary active ingredients in ginseng responsible for these effects. However, the low membrane permeability and effect on the gastrointestinal tract severely limit the absorption and bioavailability of ginsenosides [3,4].

Therefore, increasing emphasis has been placed on determining the biological activities and molecular mechanisms of primary bioactive aglycones.

Panaxadiol (PD), identified as an artificial sapogenin of ginsenosides belonging to the dammarane-type triterpene saponins formed during the process of acid hydrolysis of ginseng, attracts considerable attention due to its extensive pharmacological activities, including antitumor, radioresistance, cholesterol homeostasis, anti-Alzheimer's disease, and anti-inflammatory activities [5–8]. Although previous research has shown

that PD is an effective treatment for a variety of diseases, the underlying mechanism of PD on lung inflammation remains unknown.

Lung inflammation occurs in a variety of lung diseases and is the main cause of occurrence and aggravation of symptoms of a variety of lung diseases [9]. As the pathogen invades the body, immune cells begin to activate and phagocytose the pathogen. The activation of a large number of immune cells leads to the infiltration of various inflammatory cells, thus releasing a large number of proinflammatory mediators. Together, these inflammatory factors induce cytokine storms, which in turn induce disease or aggravate disease symptoms [10].

Typically, inhaled medications are used to treat lung diseases. Inhalation can precisely deliver drugs to the lungs and produce a local or systemic therapeutic effect without drug absorption and metabolism by the liver and intestines [11]. In addition, the large surface area, dense capillary network, and thin alveolar epidermal cell layer of the lungs are distinct benefits for systemic delivery. By concentrating the drug in the lesion, the pulmonary drug delivery system can increase drug bioavailability and stability while decreasing the first-pass effect. Significantly, its potential in clinical research for the treatment of respiratory diseases may be irreplaceable [12].

We explored the anti-inflammatory effect of PD in a mouse model of lung inflammation induced by LPS. The results showed that PD effectively reduced inflammatory cell infiltration and the production of inflammatory cytokines. Notably, inhalation administration produced the same therapeutic effects at a dose 2,000 times lower than the intragastric administration dose. PD also inhibited the production of inflammatory factors in LPS-stimulated THP-1 cells or human BALF cells. In addition, we found PD decreased the expression of TNFA/TNFAR and IL7/IL7R, as determined by RNA sequencing. TNFA and IL7 reversed the inhibition of the JAK1 signaling pathway and blocked the antiapoptotic effects of PD in a coculture model of epithelial cells and macrophages, which was further validated in a human BALF cell experiment. These results suggest PD can reduce macrophage-driven inflammation and induce epithelial apoptosis through the TNFA/TNFAR and IL7/IL7R pathways and can be used in the treatment of lung inflammation.

2. Materials and methods

2.1. Animals

25 g Mice and 200 g rats were purchased from Shanghai Slack Laboratory Animal Co., Ltd. (certificate: SCXK 2022-0012, Shanghai, China). All animals were housed in individually ventilated cages (IVC) at $22 \pm 2 \,^{\circ}C$ with 40-70% humidity under a 12:12 h light/dark photocycle and fed and watered ad libitum. All experimental procedures were approved by the Animal Care and Use Committee at Zhejiang University. All efforts were made to minimize animals' suffering and to reduce the number of animals used.

2.2. Reagents and antibodies

Panaxadiol (PD, purity > 98%, the chemical structure is shown in Fig. 1A) was extracted by Professor Zhao, Yuqing's group at the Shenyang Pharmaceutical University (Shenyang, China) and was tested free of endotoxin. Enzyme-linked immunosorbent assay (ELISA) kits for tumor necrosis factor TNFA, IL1β and IL6 were purchased from Beijing 4A Biotech Co., Ltd. (Beijing, China). Reagent and antibody information is shown in Supplementary Materials Table SI.

2.3. Establishment of an LPS-induced lung inflammation model

Animals were randomly divided into 8 groups (n = 6 in each group): control (sterile saline [0.9% NaCl]), LPS (50 μg/mouse), LPS + PD (2, 10 and 20 μg/kg, inhalation [ih.]), LPS + PD (10, 50 mg/kg, gastric injection [ig.]), LPS + DEX (0.5 mg/kg, intraperitoneal injection [ip.]). In inhaled groups, mice received drugs with various concentrations in an inhalation box connected to an aerosol device (PARIBOY SX, Germany). The average amount of inhaled drugs is shown in Supplementary Materials Table SII.

Anesthetized mice were intratracheally injected with LPS (1 mg/mL in saline solution, 50 μL/mouse) through Liquid Aerosol Devices to generate a lung inflammation model (Shanghai Yuyan Instruments Co., Ltd., China). Control mice received 50 μL sterile saline intratracheally (0.9% NaCl). Treatment groups received PD or DEX 0.5 h after LPS (Fig. 1B). The inhalation groups were exposed to 10 min aerosolized PD (1, 5 and 10 mg/mL dissolved in methanol) *via* the aerosol device, while methanol for the control group. The doses were determined based on a previous study and our preliminary experiments [13].

2.4. Bronchoalveolar lavage fluid (BALF)

Mice were subjected to bronchoalveolar lavage (BAL) as described previously, and also in detail in Supplementary Materials [14]. Aseptic fiberoptic bronchoscopy was conducted to collect human BALF samples. BALF samples were obtained using fiberoptic bronchoscopy and injected into relevant lung segments in three to five room-temperature saline instillations. Liquid nitrogen preserved BALF cells for later use. BALF cells were mostly macrophages (30%) and neutrophils (30%) [15]. The protocol was approved by the Ethics Committee of the Children's Hospital of Zhejiang University School of Medicine (2022-IRB-243) and followed the guidelines of the Declaration of Helsinki. The patient information is in Supplementary Materials Table SIII.

2.5. Hematoxylin-eosin (HE) staining

Each mouse had its left upper lung fixed in 10% neutral buffered formalin for 72 h. To analyze pathological changes, lung tissues were dehydrated, embedded in paraffin, sectioned at 3 μm on a rotary microtome, and stained with H&E. Interstitial inflammation, neutrophil infiltration, congestion, and edema comprised lung injury. 0 was minimal damage, 1 slight damage, 2 moderate damage, 3 severe damage, and 4 extremely severe damage [16].

2.6. Cell culture and treatment

Human monocytic THP-1 and A549 were obtained from the Shanghai Institute of Cell Biology (Shanghai, China). THP-1 cells were cultured as described previously, and also in detail in Supplementary Materials [17]. BALF cells were cultured in RPMI 1640 (GIBCO, Grand Island, NY) containing 10% FBS (GIBCO, Grand Island, NY) in 5% CO_2 at 37 °C. BALF and THP-1 cells were treated in four groups: a control group with no treatment, a model group with 1 μg/mL LPS, a PD group with LPS and 10 μM PD, and a rescue group with 10 ng/mL IL7 or 15 ng/mL TNFA additional the PD-treatment.

2.7. Determination of cell viability by MTT assays

A549 cells in the exponential growth phase were seeded in 96-well plates at a density of 5×10^3 cells per well. The cells were exposed to collected THP-1 cell culture medium for 1, 3, and 5 days respectively. The method has been described previously, and also in detail in Supplementary Materials [18].

2.8. Flow cytometry

A549 cells in the exponential growth phase were seeded in 6-well plates with a density of 5×10^3 cells per well. The cells were exposed to collected THP-1 cell culture medium with different treatments for 24 h. Cells were collected and stained with the Annexin V-FITC Apoptosis Detection kit (40302ES20, YEASEN, China). Samples were analyzed with a CytoFLEX flow cytometer (Beckman Coulter, Germany).
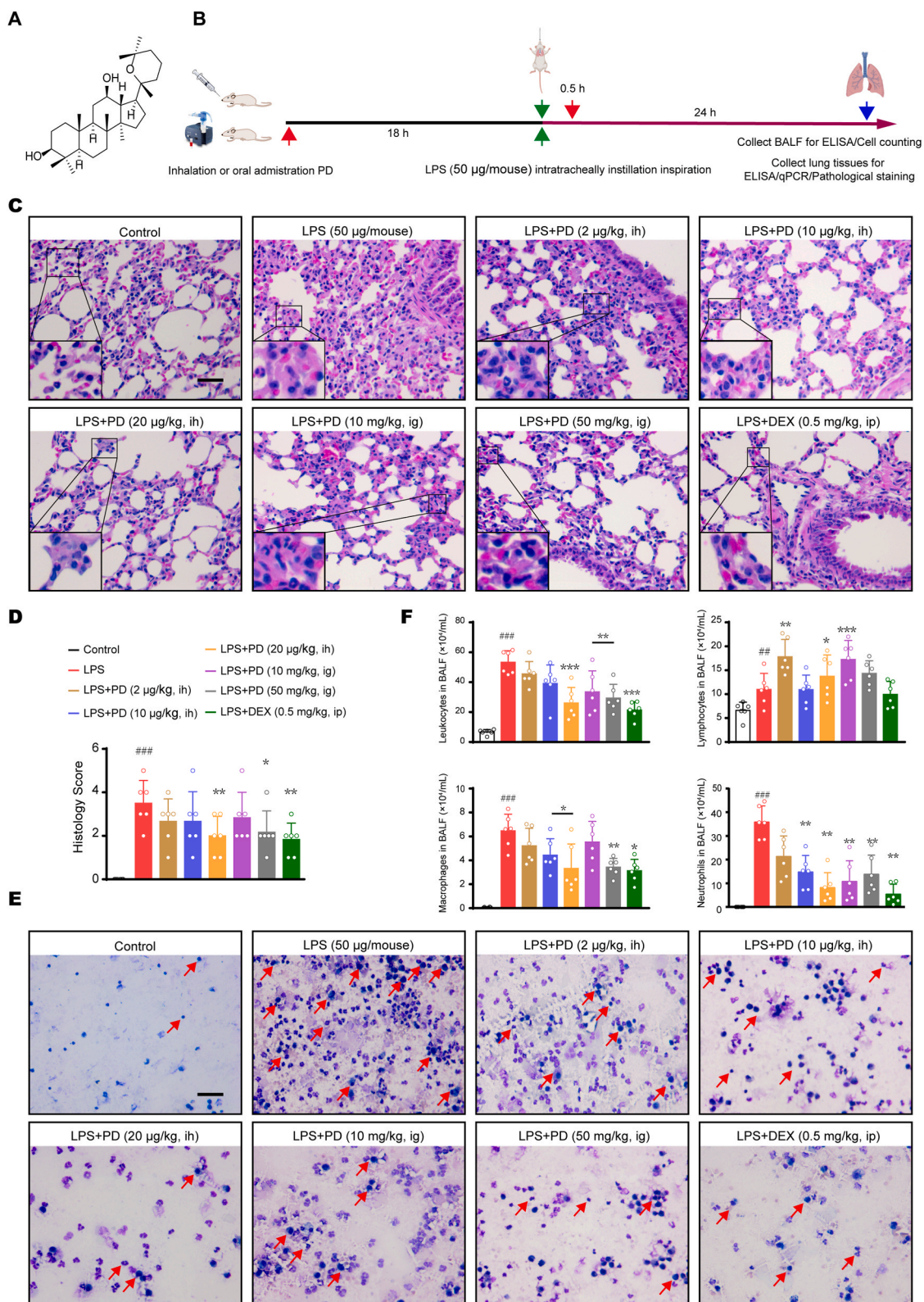
Fig. 1. Inhaled PD ameliorates LPS-induced lung pathology and inflammation.
A. The chemical structure of panaxadiol. B. Experimental pipeline is shown. C. Representative images of H&E staining of lung tissues are shown. Scale bar, 40 μm. D. Semi-quantitative histological analysis of lung tissues of 6 fields per mouse from each group is shown. E. Representative images of Wright and Giemsa staining of the BALF cells are shown. Scale bar, 40 μm. The arrows point to white blood cells. F. The counts of leukocytes, neutrophils, macrophages and lymphocytes in the BALF are quantified. The results are shown as the mean ± S.E.M., n = 6 mice per group. $^{\#\#}p < 0.01$, $^{\#\#\#}p < 0.001$ vs. control group; $^{*}p < 0.05$, $^{**}p < 0.01$, $^{***}p < 0.001$ vs. LPS group, tested by one-way ANOVA followed by Tukey's multiple comparisons.
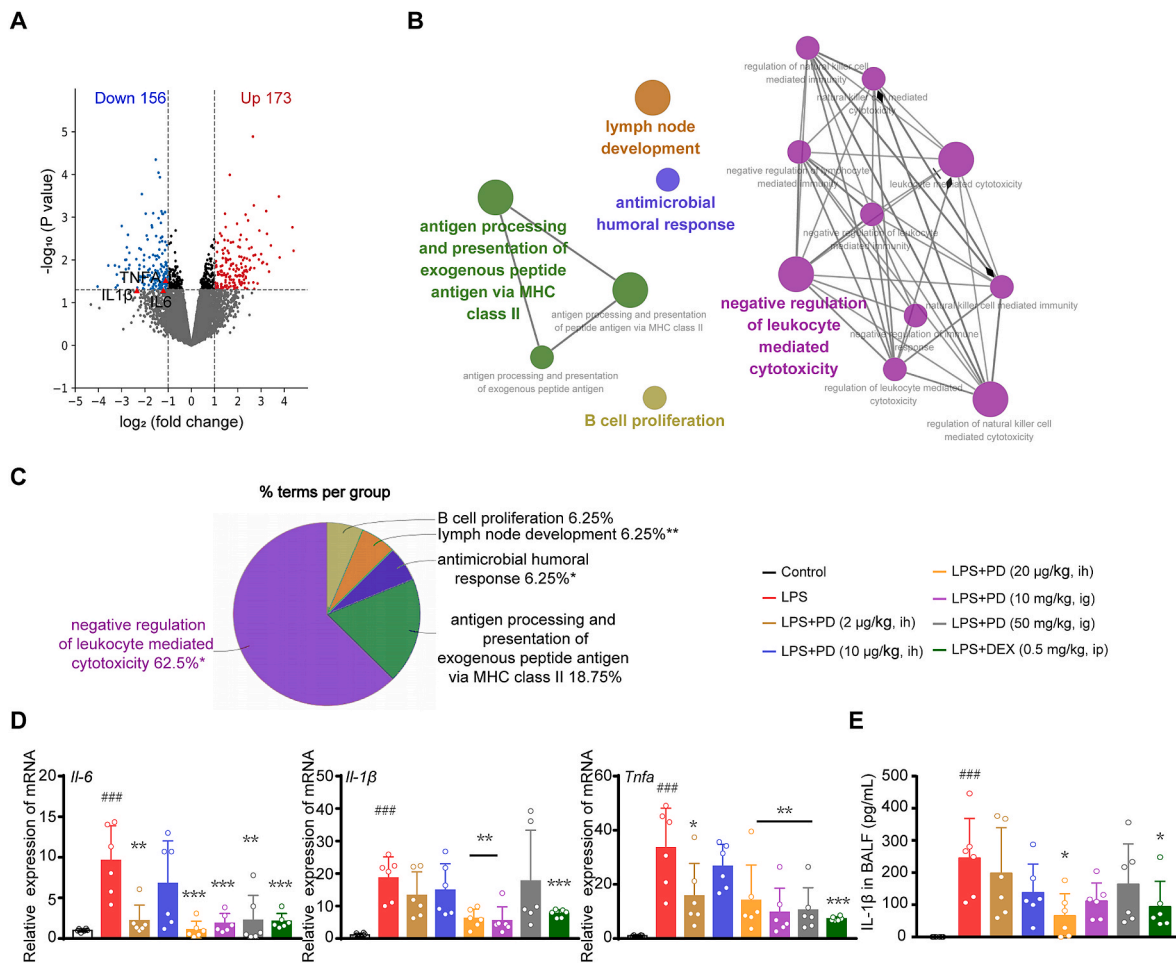
Fig. 2. Inhaled PD ameliorates the LPS-induced pneumonitis in mice.
A. Volcano plot of the DEGs for lung tissues is shown. DEGs were selected by |logFC|≥1 and pValue≤0.05. B, C Enrichment analysis of DEGs were done by Cluego: 62.5% terms are enriched in "Negative regulation of leukocyte mediated cytotoxicity". *$p < 0.05$, **$p < 0.01$, tested by Right-sided hypergeometric test. D. Relative mRNA expression of IL1β, IL6 and TNFA in lung tissues was validated by qPCR. E. The levels of IL1β in the BALF were detected by ELISA. Data are expressed as the mean ± S.E.M., n = 6 mice per group. (D, E). $^{###}p < 0.001$ vs. control group; *$p < 0.05$, **$p < 0.01$, ***$p < 0.001$ vs. LPS group, tested by one-way ANOVA followed by Tukey's multiple comparisons.

2.9. Quantitative real-time Polymerase chain reaction (RT-qPCR)

RT-qPCR experiments were performed as described previously, and also in detail in Supplementary Materials [19]. The primer sequences used in this study are listed in Supplementary Materials Table SIV.

2.10. Enzyme-linked immunosorbent assay (ELISA)

ELISA experiments were performed as described previously, and also in detail in Supplementary Materials [19].

2.11. Western blot analysis (WB)

WB experiments were performed as described previously, and also in detail in Supplementary Materials [19].

2.12. Expression profile enrichment analysis

The tissues or cells treated with PD were sent to CapitalBio Technology (Beijing, China) for NGS (next-generation sequencing). Differentially expressed genes (DEGs) were selected by |logFC|≥1 and pValue≤0.05. The volcano plot for the expression profile was depicted by our Python script.

DEG was submitted to Cluego for enrichment analysis [20].

Ontologies/Pathways for tissue enrichment is "ImmuneSystemProcess-EBI-UniProt-GOA-ACAP-ARAP" and Ontologies/Pathways for cell enrichment is "BiologicalProcess-EBI-UniProt-GOA-ACPA-ARAP". The enrichment evidence is "ALL_Experimental (EXP, IDA, IPI, IMP, IGI, IEP)". Statistical Options is Enrichment (Right-sided hypergeometric test).

2.13. Ligands and receptors matching analysis

The decrease of TNFAR (TNFRSF1A) level in lung tissues was confirmed by qPCR and was added to the DEG downregulation table of lung tissues.

Receptors in DEGs downregulation table from tissue NGS were isolated according to the receptor table from the "cell-cell interaction" database (https://baderlab.org/CellCellInteractions?action=AttachFile&do=view&target=receptors.txt). Ligands in DEGs downregulation table from cell NGS were isolated according to the ligands table from the "cell-cell interaction" database (https://baderlab.org/CellCellInteractions?action=AttachFile&do=view&target=ligands.txt). The isolation was completed by Python scripts.

Ligand and receptor pairing program was coded by Python. The receptor-ligand interaction database was downloaded from (https://baderlab.org/CellCellInteractions?action=AttachFile&do=view&target=receptor_ligand_interactions_mitab_v1.0_April2017.txt.zip).
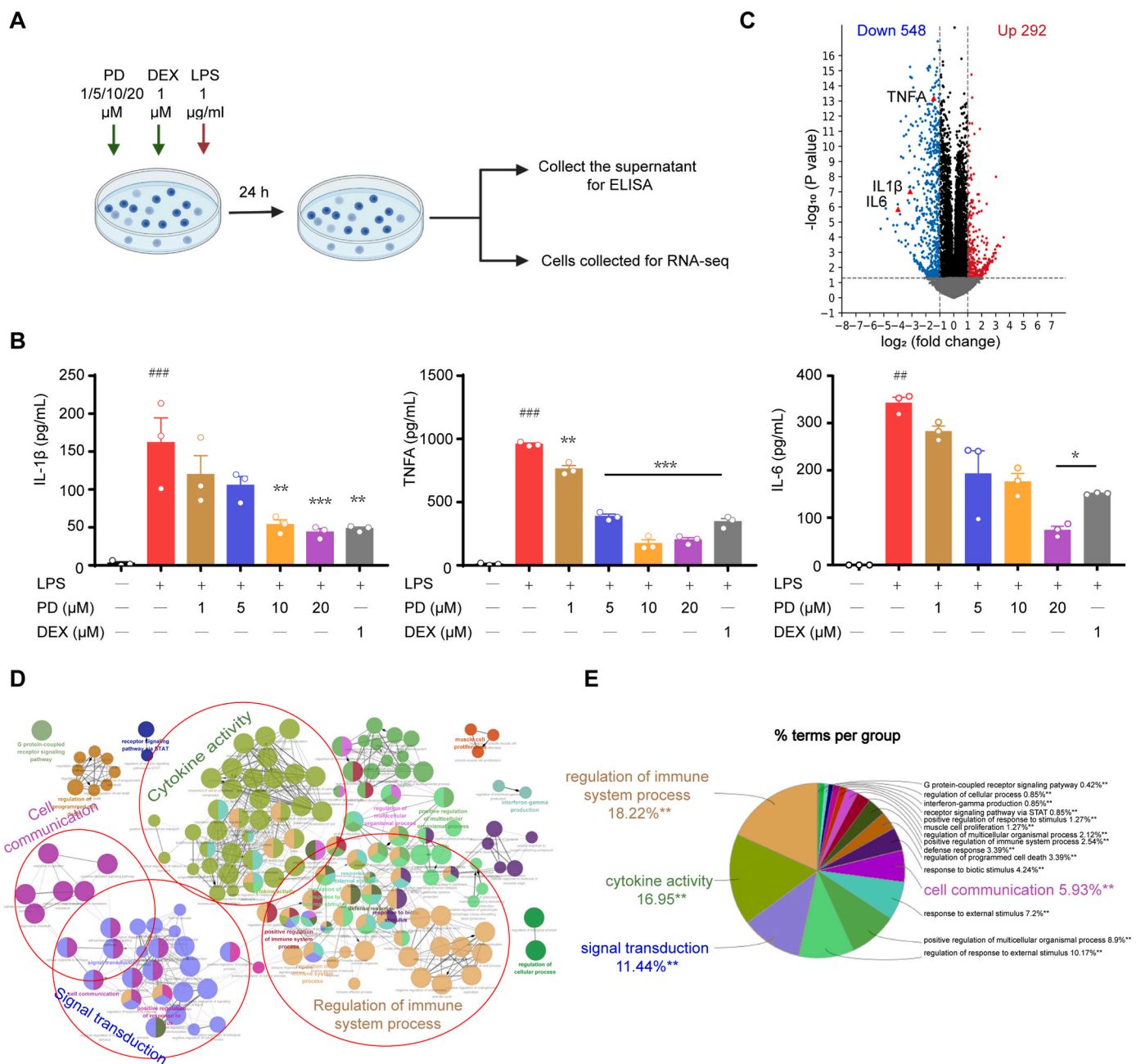
Fig. 3. PD ameliorates the LPS-induced inflammatory responses in THP-1 cells.
A. Experimental pipeline is shown. B. IL1β, IL6 and TNFA in the supernatant were detected by ELISA. The expression profile of mRNA expression was examined by NGS for the PD-treated or non-treated LPS-induced inflammatory responses in THP-1 cells. C. Volcano plot of DEGs is shown. DEGs were thresholded as $|logFC| \geq 1$ and value ≤ 0.05. D, E. Enrichment analysis of DEGs was done by Cluego. DEGs are enriched in "Cytokine activity", "Signal transduction", "Cell communication" and "Regulation of immune system process". $*p < 0.05$, $**p < 0.01$, tested by Right-sided hypergeometric test. Data are expressed as the mean ± S.E.M. of three independent experiments. (B). $^{\#\#}p < 0.01$, $^{\#\#\#}p < 0.001$ vs. control group; $*p < 0.05$, $**p < 0.01$, $***p < 0.001$ vs. LPS group, tested by one-way ANOVA followed by Tukey's multiple comparisons.

2.14. HPLC-MS/MS assay

The rats were divided into 2 groups with 9 rats for each and were administered at 3.5 mg/kg by gavage or at 0.75 mg/kg by inhalation. PD concentration determination in the lung and plasma samples utilizing a sensitive and selective liquid chromatography coupled with triple electrospray mass spectrometry (HPLC-MS/MS, AB5500, SCIEX AB, USA) mass spectrometry. Mass spectrometry fingerprint results are shown in Fig. S1.

2.15. Pharmacokinetic analysis

Pharmacokinetic parameters were calculated using DAS software (3.0, Shanghai University of Traditional Chinese Medicine, CHN) based on the blood concentration. Pharmacokinetic parameters of low, medium and high dose groups were calculated.

2.16. Statistical analysis

The results were expressed as mean ± S.E.M. Multiple intergroup comparisons were assessed by one-way analysis of variance (ANOVA)

followed by Tukey's multiple comparisons post-hoc test. Comparison between the two groups were assessed by unpaired t-test with Welch's correction. Data were analyzed by using GraphPad Prism 8.0 (San Diego, CA, USA). No samples or animals were excluded from the analysis. Experiments were performed at least in triplicates. Differences were considered significant when $p < 0.05$.

3. Results

3.1. PD inhalation ameliorates LPS-induced lung inflammation and pathology

The therapeutic effects of PD on LPS-induced lung inflammation were determined in mice (Fig. 1B). LPS-treated mice had significant morphological changes in lung tissue, including edema, hemorrhage, alveolar collapse, and neutrophil and macrophage infiltration, which were significantly improved by PD-treatment at 20 µg/kg by inhalation and 50 mg/kg by intragastric administration (Fig. 1C). Compared to intragastric administration, inhalation of PD attenuated the severity of lung pathology at a lower dose (Fig. 1D). Furthermore, the LPS-induced animal model exhibited a significant accumulation of inflammatory cells in the lungs, including macrophages, neutrophils, and lymphocytes in the BALF (Fig. 1E and F). The inflammatory cells were significantly suppressed by inhalation administration of PD at 20 µg/kg and by intragastric administration at 50 mg/kg and DEX (Fig. 1F).

Next, the pharmacokinetics of PD inhalation (0.75 mg/kg) or intragastric administration (3.5 mg/kg) were assessed in rats. Plasma drug concentrations were measured at various time points (Fig. S2A). At 24 h, PD was substantially metabolized in plasma after administration. We found inhalation resulted in a higher Cmax and AUClast, indicating inhalation administration had better drug utilization than intragastric administration (Fig. S2B, C).

3.2. LPS-induced inflammatory cytokines in the lungs are attenuated by PD inhalation

RNA-seq sequencing was used to assess the mechanisms underlying the effects of PD on lung inflammation in mice. Compared to the model group, the PD group downregulated 156 genes and upregulated 173 genes (Fig. 2A). "Negative regulation of leukocyte-mediated cytotoxicity" enriched 62.50% of the terms (Fig. 2B and C). "Antimicrobial humoral response" and "lymph node development" were also enriched. Then, the levels of inflammatory factors were examined for lung tissues. LPS significantly increased the levels of IL6, IL1β and TNFA in the BALF and lung tissues compared with the control group. The cytokines were significantly inhibited by PD treatment, particularly at a dose of 20 µg/kg by inhalation administration (Fig. 2D and E).

The proinflammatory cytokine levels in LPS-stimulated THP-1 cells were measured to assess the effects of PD (Fig. 3A). The expression of IL6, IL1β and TNFA was significantly increased after LPS stimulation and was reduced by PD in a dose-dependent manner (Fig. 3B). Next, RNA-seq was performed to investigate the mechanisms behind the effects of PD on inflammation in macrophages. Compared to the model group, PD treatment downregulated 548 genes and elevated 292 genes (Fig. 3C). Among these DEGs enriched terms, 18.22% were enriched in "regulation of immune system process", 16.95% in "cytokine activity", 11.44% in "signal transduction", and 5.93% in "cell communication" (Fig. 3D and E). Notably, numbers of viral immune pathways were enriched, including "defense response to virus", "regulation of viral life cycle", "negative regulation of viral genome replication", and "regulation of viral process". These results suggest PD may exert anti-inflammatory effects as well as antiviral function by regulating immune responses.

3.3. TNFAR, IL7R, CXCR5 and their ligands are decreased by PD-treatment in LPS-induced inflammation models

Downregulated receptors were identified in PD-treated lung tissues from the lung inflammation model in mice. Downregulated ligands were identified in the PD-treated THP-1 cells from the LPS-induced inflammation cell model (Fig. 4B and C). Using a database of ligand-receptor pairings, the identified receptors and ligands were paired (Fig. 4A). The results revealed the downregulated signaling by PD centered on three receptors (Fig. 4D), namely, TNFAR (TNFRSF1A), IL7R and CXCR5. These results suggest PD downregulated all three pathways. IL7R expresses in various organs according to NIH data (https://www.ncbi.nlm.nih.gov/gene/3575), particularly highly expresses in the lungs (Fig. 4E). In PD-treated lung tissues, the mRNA levels of all three receptors were reduced (Fig. 4F). In addition, PD-treatment also resulted in a decrease in ligands associated with these three receptors (Fig. 4F). In the in vitro models, the mRNA levels of TNFA, TNFAR, IL7R and IL7 were decreased by PD-treatment in the LPS model in A549 and THP-1 cells (Fig. 4G).

3.4. PD inhibits TNFAR and IL7R signaling in the LPS model

The effects of PD on reducing inflammation were determined in a coculture model of macrophage and epithelial cell experiments. The culture medium from THP-1 cells was applied to A549 cells to assess the effects of cytokines released by macrophage cells on epithelial cells (Fig. 5A). PD significantly reduced the increased level of TNFAR and IL7R induced by LPS. Either IL7 or TNFA supplementation increased IL7R and TNFAR at protein levels (Fig. 5B). The activation of TNFAR and IL7R initiated JAK1-mediated signaling [21]. For testing the activation of IL7/IL7R and TNFA/TNFAR signaling, the p-JAK1 level was measured in A549 cells treated with PD (Fig. 5C). The level of p-JAK1 was significantly increased in the model group, which was significantly inhibited under PD treatment. The effects of PD were blocked after the addition of IL7 or TNFA.

PD treatment decreased the apoptosis rate of A549 cells cultured in LPS-treated THP-1 medium from 17.00% to 3.02%. However, the addition of IL7, TNFA, or both enhanced the apoptosis rate in the LPS + PD group to 7.71%, 4.95%, and 8.41%, respectively. The addition of a selective JAK1 inhibitor, upadacitinib, in LPS + PD + IL7+TNFA group reduced the apoptosis rate from 8.41% to 4.27% (Fig. 5D). Interestingly, PD also increased the proliferation rate of A549 cells treated with the medium from LPS-treated THP-1 cells, which were reversed by addition of IL7 or IL7 and TNFA (Fig. 5E). In addition, the JAK1 inhibitor also increased the proliferation rate of the LPS + PD + IL7+TNFA group on the 5th day (Fig. 5E).

3.5. PD protects epithelial cells by suppressing inflammation in a human BALF cell model

The anti-inflammatory effects of PD were validated in human BALF cells (Fig. 6A). Consistently, LPS significantly increased the levels of IL6, IL1β and TNFA in the BALF cells compared with the control group, which were significantly suppressed by PD (Fig. 6B). Subsequently, the culture medium from BALF cells was applied to A549 cells to assess the effects of the factors released from the BALF cells on epithelial cells. PD reduced the apoptosis rate of A549 cells cultured in LPS-treated BALF cell medium from 12.44% to 4.70%, which were reversed to 4.70% to 6.6%, 5.44%, and 9.02% by the addition of IL7, TNFA or IL7 and TNFA, respectively (Fig. 6C).

4. Discussion

Lung inflammation is the main cause of the occurrence and aggravation of symptoms in a variety of lung diseases [10,22,23]. In this study, we found inhalation administration of PD was more effective than
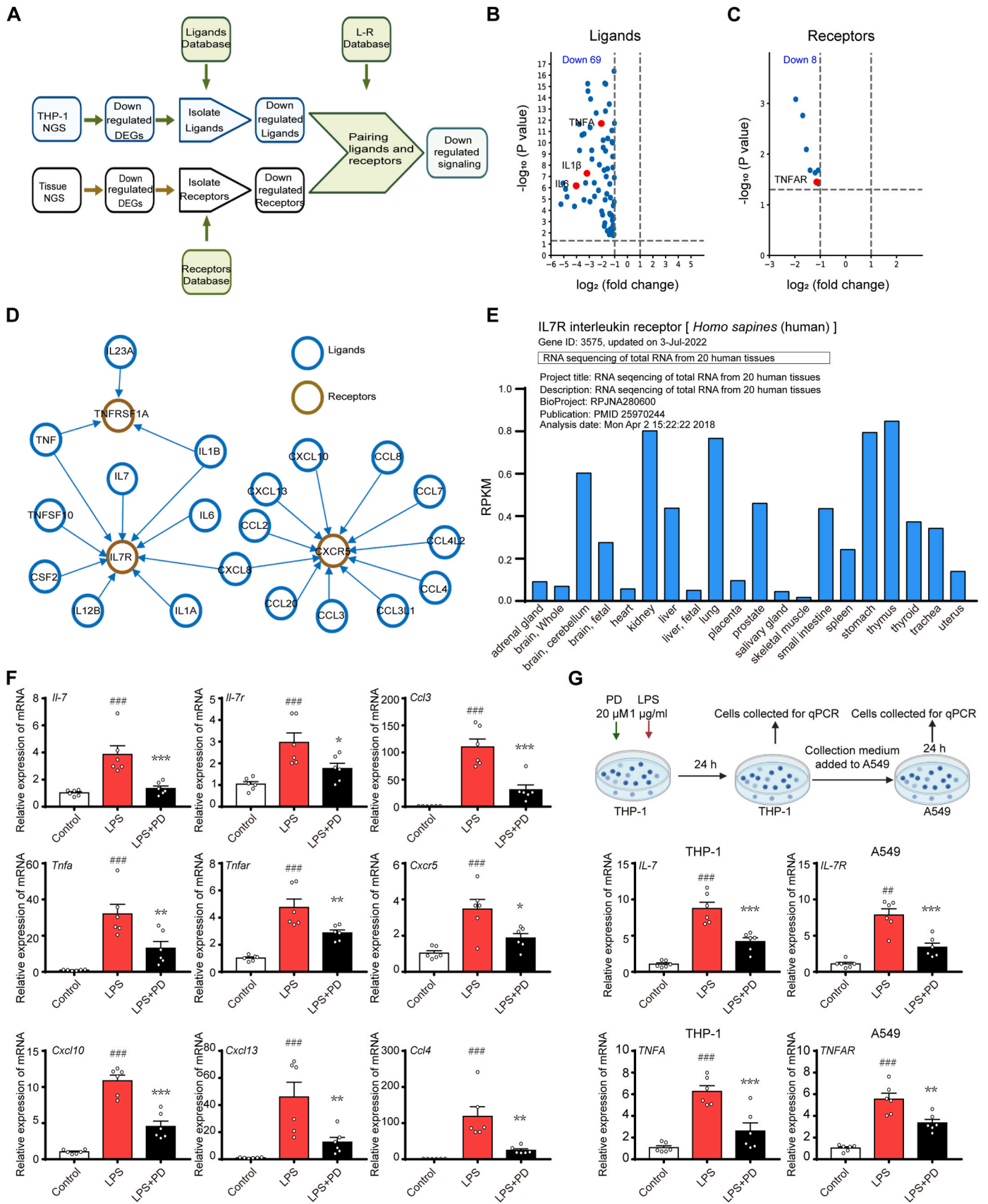
(caption on next page)

Fig. 4. PD may inhibit the interactions between macrophages (THP1) and epithelial cells (A549) *via* suppression of TNFA and IL7 signaling. A. The pipeline of cell-cell interaction bioinformatics analysis is shown. Down-regulated DEGs from the mouse model were used to screen receptors and down-regulated DEGs from the cell model were used to screen down-regulated ligands. Ligand-receptor pairs were determined. B. Down-regulated ligands in the cell culture model (THP-1) treated by PD are shown. C. Down-regulated receptors in the mouse model treated by PD are shown. D. The pairing results of PD-induced downregulated ligands and receptors are shown. The lines stand for the interactions. The arrows stand for binding direction. TNFRSF1A is the formal symbol of TNFAR. E. IL7R RNA expression profile in different organs is shown. Data is from NIH (https://www.ncbi.nlm.nih.gov/gene/3575). F. Relative mRNA expression of various genes in lung tissues in the LPS-induced mouse model was assessed by qPCR. G. Relative mRNA expression of TNFA and TNFAR in the model of THP-1 and A549 cells was assessed by qPCR respectively. Data are expressed as the mean ± S.E.M., n = 6 mice or 6 independent experiments per group. $^{\#\#}p < 0.01$, $^{\#\#\#}p < 0.001$ vs. control group; $^{*}p < 0.05$, $^{**}p < 0.01$, $^{***}p < 0.001$ vs. LPS group, tested by one-way ANOVA followed by Tukey's multiple comparisons.

intragastric administration at reducing inflammatory cell infiltration and inflammatory cytokine production in mice with LPS-induced lung inflammation. PD also suppressed the production of inflammatory factors in THP-1 cells or human BALF cells stimulated by LPS. RNA-seq analysis revealed PD inhibits the expression of TNFA/TNFAR and IL7/IL7R. Indeed, TNFA and IL7 reversed the inhibition of the JAK1 signaling pathway and blocked the anti-apoptotic effects of PD in a coculture model of epithelial cells and macrophages. These results suggest PD can reduce macrophage-driven inflammation and its induced apoptosis in epithelial cells through the TNFA/TNFAR and IL7/IL7R pathways, which can be used to treat severe symptoms in diseases with lung inflammation.

The primary pathogenic mechanism of lung disease is characterized as excessive inflammatory responses [24,25]. Pulmonary infections result in the invasion of inflammatory cells and the release of pro-inflammatory mediators, which accelerate the production and release of inflammatory factors by binding to various receptors, causing a cytokine storm [26]. Macrophages play a key role in the inflammatory response of lung inflammation [22]. In response to foreign pathogens, they secrete several inflammatory factors and chemokines, which initiate the chain reaction of inflammatory reactions and cause lung tissue damage [27–29]. Our findings that PD inhibited the release of inflammatory factors from LPS-stimulated THP-1 cells and human BALF cells indicate PD has therapeutic effects in suppressing inflammation.

Recent research shows it is important for diagnosis and treatment to understand how the interactions between cells cause illness [30–32]. Alveolar macrophages (AMs) and alveolar epithelial cells (AECs) are the first cells contacting with pathogens and destroy them with limited damage to the lungs [33]. Through ligand-receptor interactions, CD200R, PD-1, and SIRP1 on AMs and CD200, PDL-1, and CD47 on AECs maintain quiescence in a steady-state microenvironment [34,35]. The relationship between AECs and AMs can change in the presence of inflammation, hypoxia, infection, and fibrosis, which in turn affects the progression of the disease [36–39]. We investigated the mRNA expression profile of PD-treated lung tissues and THP-1 cells in LPS-induced models to understand the full picture of changes at the transcriptional level by RNA sequencing and analysis. We found 62.5% of DEGs enriched terms were enriched in "negative regulation of leukocyte-mediated cytotoxicity" in the tissue expression profile. This suggests PD can improve lung inflammation by "negative regulation of leukocyte-mediated cytotoxicity". In the THP-1 expression profile, DEGs were enriched in "cytokine activity", "signal transduction", "cell communication" and "immune system process regulation". The elevated number of DEGs in these four groups indicates PD may regulate cytokine signaling in the lung inflammation models in AECs and AMs. To study the relationship between AECs and AMs, we used a coculture model of epithelial cells and macrophages in which THP-1 cells and A549 cells were used to simulate the conditions of AMs and AECs, respectively. We found PD reduced the amount of apoptosis of A549 cells that were administered the supernatant of THP-1 cells treated with LPS. Previous

studies have shown that AEC apoptosis aggravates lung inflammation and damage in multiple lung diseases, such as hypoxia/reoxygenation-induced injury, fibrosis, and chronic obstructive pulmonary disease [40]. These results suggest PD may ameliorate the alteration of the cell-to-cell connection between AECs and AMs, which results in reduced apoptosis of AECs and lung inflammation.

To further understand the effects of PD on cell-to-cell interactions in lung inflammation, we investigated the downregulated pairs of ligands and receptors in THP-1 cells and lung tissues. Although more ligands were found, only three receptors were found in the investigation, namely, TNFAR, IL7R and CXCR5. TNFAR and IL7R are single trans-membrane receptors, whereas CXCR5 has seven transmembrane domains. IL7R is mostly found on B and T cells, where it facilitates their growth and sustains their survival. IL7R is expressed in lung tissues, and its expression level is positively correlated with the number of immune cells in the lungs [41]. We found PD decreased the levels of TNFA/TNFAR and IL7/IL7R in models of lung inflammation *in vivo* and *in vitro*. Interestingly, PD suppressed p-JAK1 in a coculture model of epithelial cells and macrophages. p-JAK1 has been shown to be the downstream signal of IL7R and TNFAR activation [21,42]. The addition of IL7 and TNFA reversed the inhibition of p-JAK1 by PD and blocked the amelioration of apoptosis in A549 cells. These results proved the bioinformatics prediction that PD blocks IL7/IL7R and TNFA/TNFAR signaling. The role of IL7 in promoting or inhibiting apoptosis is still controversial. It was reported that IL7 can prevent T-cells and NK cells from apoptosis [43,44]. However, IL7 also can promote B cell apoptosis, and induce cardiomyocyte apoptosis through macrophages [45,46]. In our study, IL7 induced lung epithelial cells (A549) apoptosis induced by macrophages activation which can be inhibited by PD. In summary, our results suggest PD decreases apoptosis in epithelial cells through the suppression of the TNFA/TNFAR and IL7/IL7R pathways between macrophages and epithelial cells, which may contribute to the alleviation of severe symptoms in mouse models of lung inflammation.

Inhalation is one of the most important ways to administer medicine to people with lung diseases. Inhalation enables the medicine to travel directly to the lungs, which can boost drug use and enhance therapeutic effects [47]. Our study found that achieving the same efficacy by inhalation was 2,000 times lower than the intragastric administration dose. Pharmacokinetics showed higher Cmax and AUClast values for inhalation administration at 4.6 times lower doses, suggesting inhalation can be used to achieve efficacy with less drug exposure.

In this study, we found that inhaled PD had better therapeutic effects compared to conventional administration. PD was effective in treating lung inflammation by inhibiting TNFA/TNFAR and IL7/IL7R pathways between macrophages and epithelial cells. We provide a drug candidate and suggest a more effective administration route for ginseng and its derivatives in the treatment of lung inflammation.
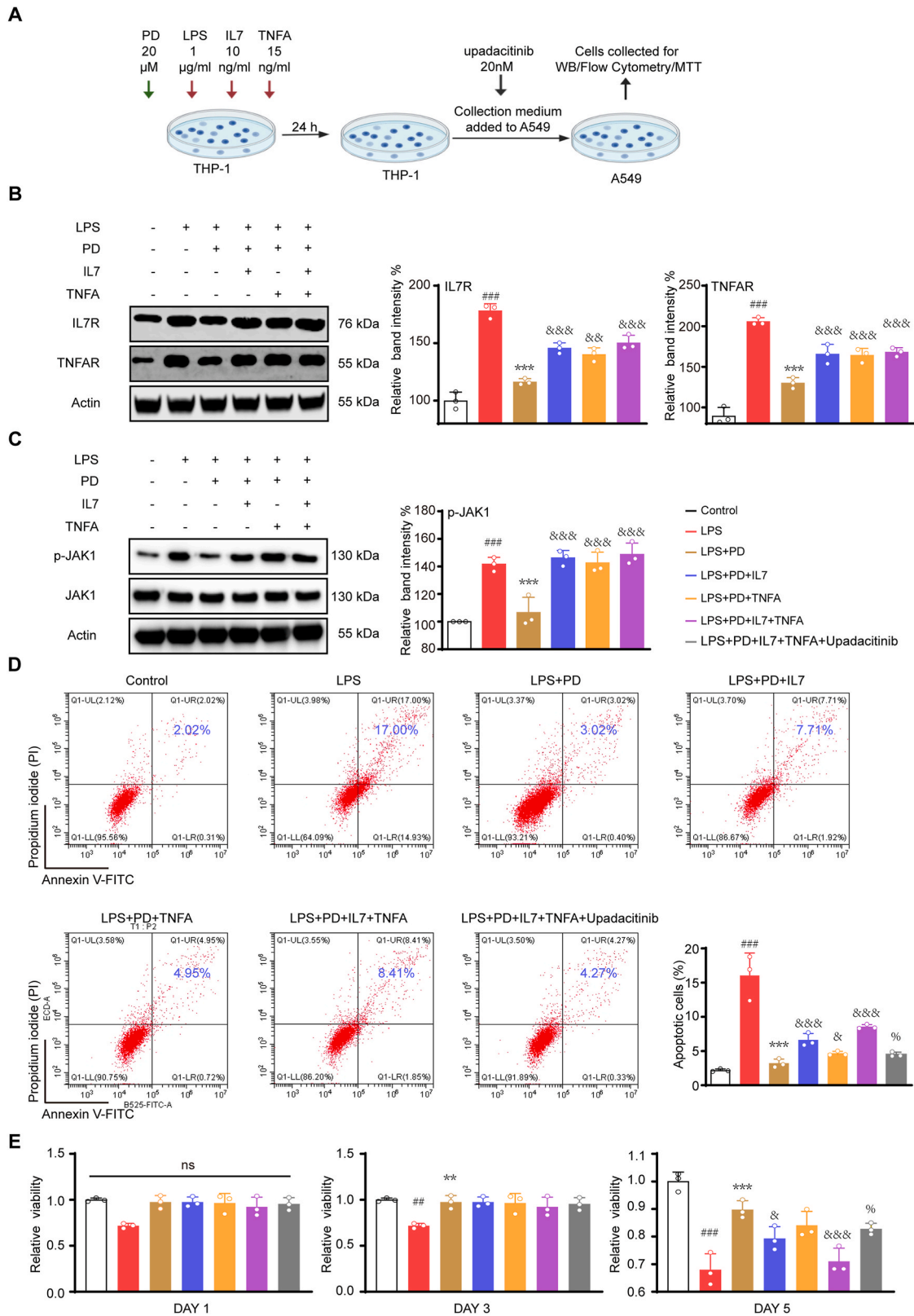
Fig. 5. PD promotes the survival rate of epithelial cells *via* inhibiting TNFAR and IL7R signaling pathways in a LPS-induced THP-1 and epithelial cell coculture model.

A. Experimental pipeline is shown. B. The protein levels of IL7R and TNFAR in A549 cells treated with 1 h of THP-1 culture medium. C. The protein levels of p-JAK1 and JAK1 in A549 cells treated with 15 min of THP-1 culture medium. The left picture showed the legend for each group. This is not specifically for C but for all the bar charts in Fig. 5. D. The apoptosis of A549 cells cultured with THP-1 culture medium in 24 h were determined by flow cytometry. The concentration of upadacitinib in the cell medium was 20 nM. E. The proliferation of A549 cells 1, 3, and 5 days after culturing with THP-1 cell culture medium is shown. The concentration of upadacitinib in the cell medium was 20 nM. Data are expressed as the mean ± S.E.M. of three independent experiments (B, C, D, E). ###$p < 0.001$ vs. control group; **$p < 0.01$, ***$p < 0.001$ vs. LPS group; &$p < 0.05$, &&&$p < 0.001$ vs. LPS + PD group, tested by one-way ANOVA followed by Tukey's multiple comparisons, %$p < 0.05$ vs. LPS + PD + IL7+TNFA group.''
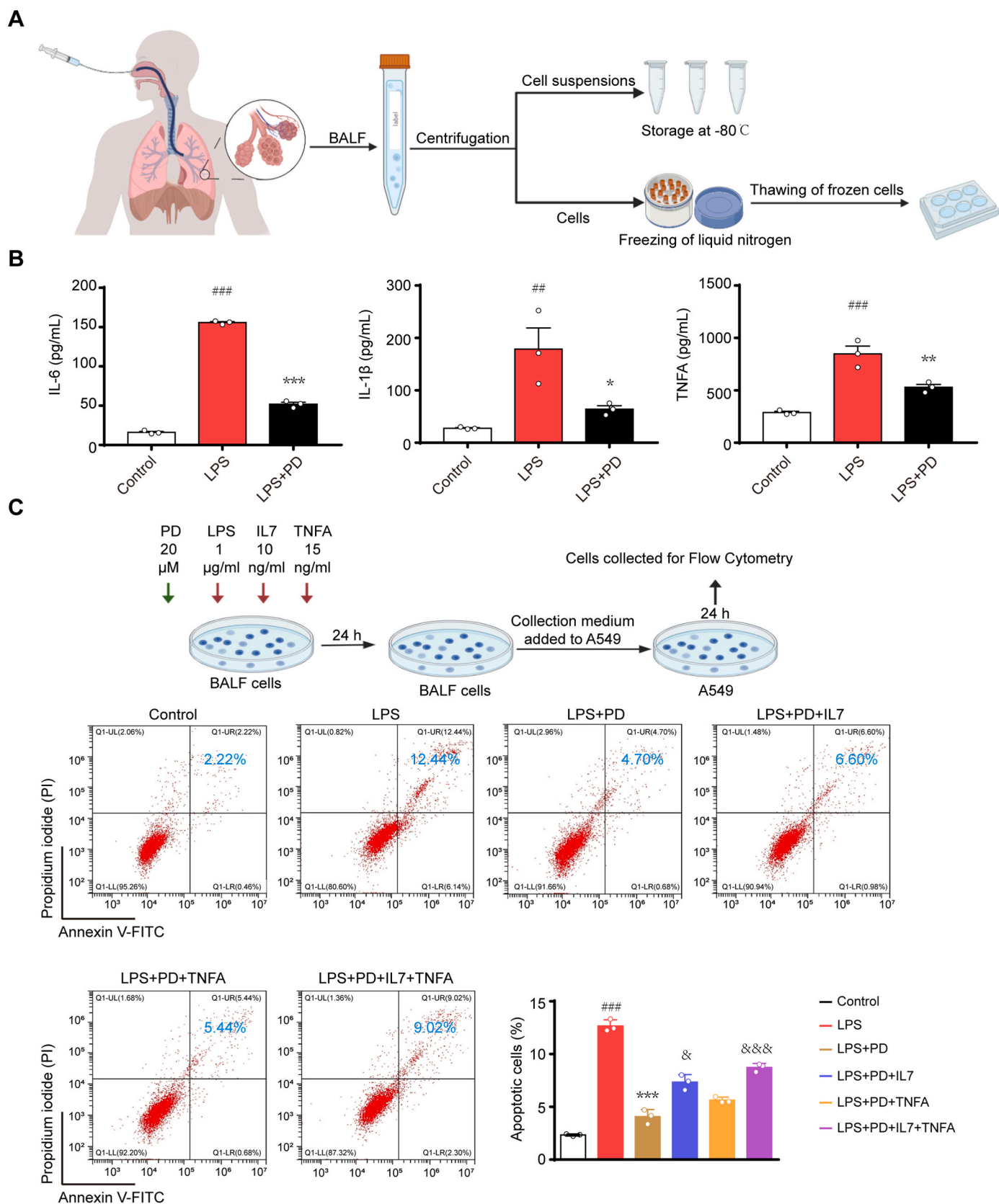
Fig. 6. PD promotes the survival rate of epithelial cells *via* inhibiting TNFAR and IL7R signaling pathways in a LPS-induced human BALF and epithelial coculture model.

A. Flow chart of the acquisition of human BALF cells is demonstrated. B. The protein levels of IL1β, IL6 and TNFA in the supernatant were assessed by ELISA. C. The apoptosis of A549 cells cultured with medium from the LPS-treated BALF cells for 24 h were assessed by flow cytometry. Data are expressed as the mean ± S.E.M. of three independent experiments. ##$p < 0.01$, ###$p < 0.001$ vs. control group; *$p < 0.05$, **$p < 0.01$, ***$p < 0.001$ vs. LPS group; &$p < 0.05$, &&&$p < 0.001$ vs. LPS + PD group, tested by one-way ANOVA followed by Tukey's multiple comparisons.

Declarations

Consent for publication

All the consent of participants were acquired.

Funding

Authors' contributions

YX, YW and QS conceived and designed the study. YW and HW performed the experiments and analyzed the results. XL participated in experiments and analyzed the results. ZS performed all the bioinformatical analyses. YX, YW and HW wrote and revised the manuscript. LJ and MZ performed the pharmacokinetic experiment. SL, WL, YZ and LW provided experimental resources and participated in the experimental data acquisition, analysis and interpretation. YX, LW, HS and SL provided funding support.

Declaration of competing interest

The authors whose names are listed immediately below certify that they have NO affiliations with or involvement in any organization or entity with any financial interest (such as honoraria; educational grants; participation in speakers' bureaus; membership, employment, consultancies, stock ownership, or other equity interest; and expert testimony or patent-licensing arrangements), or nonfinancial interest (such as personal or professional relationships, affiliations, knowledge or beliefs) in the subject matter or materials discussed in this manuscript.

Acknowledgements

Appendix A. Supplementary data

Supplementary data to this article can be found online at https://doi.org/10.1016/j.jgr.2023.09.002.

References

[1] Cui S, Wu J, Wang J, Wang X. Discrimination of American ginseng and Asian ginseng using electronic nose and gas chromatography-mass spectrometry coupled with chemometrics. J Ginseng Res 2017;41:85–95.
[2] Boonlert W, Benya AH, Umka WJ, Rodsiri R. Ginseng extract G115 attenuates ethanol-induced depression in mice by increasing brain BDNF levels. Nutrients 2017;9.
[3] Tawab MA, Bahr U, Karas M, Wurglics M, Schubert-Zsilavecz M. Degradation of ginsenosides in humans after oral administration. Drug Metab Dispos 2003;31:1065–71.
[4] Hsu BY, Lu TJ, Chen CH, Wang SJ, Hwang LS. Biotransformation of ginsenoside Rd in the ginseng extraction residue by fermentation with lingzhi (Ganoderma lucidum). Food Chemistry 2013;141:4186–93.
[5] Lin XH, Cao MN, He WN, Yu SW, Guo DA, Ye M. Biotransformation of 20(R)-panaxadiol by the fungus Rhizopus chinensis. Phytochemistry 2014;105:129–34.
[6] Lee HJ, Kim SR, Kim JC, Kang CM, Lee YS, Jo SK, Kim TH, Jang JS, Nah SY, Kim SH. *In Vivo* radioprotective effect of Panax ginseng C.A. Meyer and identification of active ginsenosides. Phytother Res 2006;20:392–5.
[7] Liang X, Yao Y, Lin Y, Kong L, Xiao H, Shi Y, Yang J. Panaxadiol inhibits synaptic dysfunction in Alzheimer's disease and targets the Fyn protein in APP/PS1 mice and APP-SH-SY5Y cells. Life Sci 2019;221:35–46.
[8] Kwon BM, Kim MK, Baek NI, Kim DS, Park JD, Kim YK, Lee HK, Kim SI. Acyl-CoA: cholesterol acyltransferase inhibitory activity of ginseng sapogenins, produced from the ginseng saponins. Bioorg Med Chem Lett 1999;9:1375–8.
[9] Quinton LJ, Walkey AJ, Mizgerd JP. Integrative physiology of pneumonia. Physiol Rev 2018;98:1417–64.
[10] Scherer PM, Chen DL. Imaging pulmonary inflammation. J. Nucl. Med. : Official Publication, Society of Nuclear Medicine 2016;57:1764–70.
[11] Zhang G, Mo S, Fang B, Zeng R, Wang J, Tu M, Zhao J. Pulmonary delivery of therapeutic proteins based on zwitterionic chitosan-based nanocarriers for treatment on bleomycin-induced pulmonary fibrosis. Int J Biol Macromol 2019;133:58–66.
[12] Thakur AK, Chellappan DK, Dua K, Mehta M, Satija S, Singh I. Patented therapeutic drug delivery strategies for targeting pulmonary diseases. Expert Opinion on Therapeutic Patents 2020;30:375–87.
[13] Li J, Lu K, Sun F, Tan S, Zhang X, Sheng W, Hao W, Liu M, Lv W, Han W. Panaxydol attenuates ferroptosis against LPS-induced acute lung injury in mice by Keap1-Nrf2/HO-1 pathway. J. Translat. Med. 2021;19:1–14.
[14] Xie YC, Dong XW, Wu XM, Yan XF, Xie QM. Inhibitory effects of flavonoids extracted from licorice on lipopolysaccharide-induced acute pulmonary inflammation in mice. Int. Immunoph. 2009;9:194–200.
[15] Rankin JA, Marcy T, Rochester CL, Sussman J, Smith S, Buckley P, Lee D. Human airway macrophages. A technique for their retrieval and a descriptive comparison with alveolar macrophages. Am Rev Respir Dis 1992;145:928–33.
[16] Zhang C, Li W, Li X, Wan D, Mack S, Zhang J, Wagner K, Wang C, Tan B, Chen J. Novel aerosol treatment of airway hyper-reactivity and inflammation in a murine model of asthma with a soluble epoxide hydrolase inhibitor. PloS One 2022;17:e0266608.
[17] Gao S, Hu J, Wu X, Liang Z. PMA treated THP-1-derived-IL-6 promotes EMT of SW48 through STAT3/ERK-dependent activation of Wnt/beta-catenin signaling pathway. Biomed Pharmacother 2018;108:618–24.
[18] Tonder A, Joubert AM, Cromarty AD. Limitations of the 3-(4,5-dimethylthiazol-2-yl)-2,5-diphenyl-2H-tetrazolium bromide (MTT) assay when compared to three commonly used cell enumeration assays. BMC Res Notes 2015;8:47.
[19] Gong L, Zhu T, Chen C, Xia N, Yao Y, Ding J, Xu P, Li S, Sun Z, Dong X, et al. Miconazole exerts disease-modifying effects during epilepsy by suppressing neuroinflammation via NF-kappaB pathway and iNOS production. Neurobiol Dis 2022;172:105823.
[20] Bindea G, Mlecnik B, Hackl H, Charoentong P, Tosolini M, Kirilovsky A, Fridman WH, Pages F, Trajanoski Z, Galon J. ClueGO: a Cytoscape plug-in to decipher functionally grouped gene ontology and pathway annotation networks. Bioinformatics 2009;25:1091–3.
[21] Liu Y, Easton J, Shao Y, Maciaszek J, Wang Z, Wilkinson MR, McCastlain K, Edmonson M, Pounds SB, Shi L, et al. The genomic landscape of pediatric and young adult T-lineage acute lymphoblastic leukemia. Nat Genet 2017;49:1211–8.
[22] Fan EKY, Fan J. Regulation of alveolar macrophage death in acute lung inflammation. Respir Res 2018;19:50.
[23] Cosio MG, Guerassimov A. Chronic obstructive pulmonary disease. Inflammation of small airways and lung parenchyma. Am. J. Respirat. Critical Care Med. 1999;160:S21–5.
[24] Liu C, Xiao K, Xie L. Progress in preclinical studies of macrophage autophagy in the regulation of ALI/ARDS. Front Immunol 2022;13:922702.
[25] Mokra D, Kosutova P. Biomarkers in acute lung injury. Respir Physiol Neurobiol 2015;209:52–8.
[26] Thompson BT, Chambers RC, Liu KD. Acute respiratory distress syndrome. N Engl J Med 2017;377:562–72.
[27] Byrne AJ, Mathie SA, Gregory LG, Lloyd CM. Pulmonary macrophages: key players in the innate defence of the airways. Thorax 2015;70:1189–96.
[28] Yu X, Buttgereit A, Lelios I, Utz SG, Cansever D, Becher B, Greter M. The cytokine TGF-beta promotes the development and homeostasis of alveolar macrophages. Immunity 2017;47:903–912 e4.
[29] Huang X, Xiu H, Zhang S, Zhang G. The role of macrophages in the pathogenesis of ALI/ARDS. Mediators Inflamm 2018;2018:1264913.
[30] Li W, Li D, Chen Y, Abudou H, Wang H, Cai J, Wang Y, Liu Z, Liu Y, Fan H. Classic signaling pathways in alveolar injury and repair involved in sepsis-induced ALI/ARDS: new research progress and prospect. Dis Markers 2022;2022:6362344.
[31] Luh SP, Chiang CH. Acute lung injury/acute respiratory distress syndrome (ALI/ARDS): the mechanism, present strategies and future perspectives of therapies. J Zhejiang Univ Sci B 2007;8:60–9.
[32] Mohan A, Agarwal S, Clauss M, Britt NS, Dhillon NK. Extracellular vesicles: novel communicators in lung diseases. Respir Res 2020;21:175.
[33] Gschwend J, Sherman SPM, Ridder F, Feng X, Liang HE, Locksley RM, Becher B, Schneider C. Alveolar macrophages rely on GM-CSF from alveolar epithelial type 2 cells before and after birth. J Exp Med 2021:218.
[34] Bissonnette EY, Lauzon JJF, Debley JS, Ziegler SF. Cross-talk between alveolar macrophages and lung epithelial cells is essential to maintain lung homeostasis. Front Immunol 2020;11:583042.
[35] Tao H, Xu Y, Zhang S. The role of macrophages and alveolar epithelial cells in the development of ARDS. Inflammation 2023;46:47–55.
[36] Mu M, Gao P, Yang Q, He J, Wu F, Han X, Guo S, Qian Z, Song C. Alveolar epithelial cells promote IGF-1 production by alveolar macrophages through TGF-beta to suppress endogenous inflammatory signals. Front Immunol 2020;11:1585.

[37] Baloglu E, Velineni K, Ermis KE, Mairbaurl H. Hypoxia aggravates inhibition of alveolar epithelial Na-transport by lipopolysaccharide-stimulation of alveolar macrophages. Int. J. Molecul. Sci. 2022;23.

[38] Sadikot RT, Bedi B, Li J, Yeligar SM. Alcohol-induced mitochondrial DNA damage promotes injurious crosstalk between alveolar epithelial cells and alveolar macrophages. Alcohol 2019;80:65–72.

[39] Du J, Li G, Jiang L, Zhang X, Xu Z, Yan H, Zhou Z, He Q, Yang X, Luo P. Crosstalk between alveolar macrophages and alveolar epithelial cells/fibroblasts contributes to the pulmonary toxicity of gefitinib. Toxicol Lett 2021;338:1–9.

[40] Conlon TM, Schuster JG, Heide D, Pfister D, Lehmann M, Hu Y, Ertuz Z, Lopez MA, Ansari M, Strunz M, et al. Inhibition of LTbetaR signalling activates WNT-induced regeneration in lung. Nature 2020;588:151–6.

[41] Wang X, Chang S, Wang T, Wu R, Huang Z, Sun J, Liu J, Yu Y, Mao Y. IL7R is correlated with immune cell infiltration in the tumor microenvironment of lung adenocarcinoma. Front Pharmacol 2022;13:857289.

[42] Guo D, Dunbar JD, Yang CH, Pfeffer LM, Donner DB. Induction of Jak/STAT signaling by activation of the type 1 TNF receptor. J Immunol 1998;160:2742–50.

[43] Li WQ, Jiang Q, Khaled AR, Keller JR, Durum SK. Interleukin-7 inactivates the pro-apoptotic protein Bad promoting T cell survival. Journal of Biological Chemistry 2004;279:29160–6.

[44] Armant M, Delespesse G, Sarfati M. IL-2 and IL-7 but not IL-12 protect natural killer cells from death by apoptosis and up-regulate bcl-2 expression. Immunology 1995;85:331.

[45] Sammicheli S, Dang Vu Phuong L, Ruffin N, Pham Hong T, Lantto R, Vivar N, Chiodi F, Rethi B. IL-7 promotes CD95-induced apoptosis in B cells via the IFN-γ/STAT1 pathway. PloS One 2011;6:e28629.

[46] Yan M, Yang Y, Zhou Y, Yu C, Li R, Gong W, Zheng J. Interleukin-7 aggravates myocardial ischaemia/reperfusion injury by regulating macrophage infiltration and polarization. J Cell Mol Med 2021;25:9939–52.

[47] Patton JS, Byron PR. Inhaling medicines: delivering drugs to the body through the lungs. Nat Rev Drug Discov 2007;6:67–74.